

The morphology and surface features

T. J. Jones et al.

The morphology and surface features of olivine in kimberlite lava: implications for ascent and emplacement mechanisms

T. J. Jones^{1,2}, J. K. Russell¹, L. A. Porritt^{1,2}, and R. J. Brown³

¹Department of Earth, Ocean and Atmospheric Sciences, University of British Columbia, Vancouver, V6T 1 Z4, Canada

²School of Earth Sciences, University of Bristol, Wills Memorial Building, Bristol, BS8 1RJ, UK

³Department of Earth Sciences, Science Labs, Durham University, Durham, DH1 3LE, UK

Received: 26 November 2013 – Accepted: 29 November 2013 – Published: 13 December 2013

Correspondence to: T. J. Jones (thomas.jones.2010@my.bristol.ac.uk)

Published by Copernicus Publications on behalf of the European Geosciences Union.

Title Page

Abstract

Introduction

Conclusions

References

Tables

Figures

◀

▶

◀

▶

Back

Close

Full Screen / Esc

Printer-friendly Version

Interactive Discussion



Abstract

Many kimberlite rocks contain large proportions of ellipsoidal-shaped xenocrystic olivine grains that are derived mainly from the disaggregation of peridotite. Xenocrystic olivine grains from a lava erupted from the Quaternary Igwisi Hills kimberlites, Tanzania, are compared to phenocrystic olivine, liberated from picritic lavas, and mantle olivine, liberated from a fresh peridotite xenolith, in order to examine the potential modification of olivine surface textures due to transport from the mantle to the surface within kimberlite magmas. Image analysis, SEM imagery and laser microscopy reveals significant differences in the surface features and morphologies of the three crystal populations. Xenocrystic olivine grains are characterised by rough surfaces, ellipsoidal shapes and impact pits. Mantle olivines are characterised by flaked surfaces and indented shapes consistent with growth as a crystal aggregates. Phenocrystic olivines are smooth-surfaced and exhibit flat crystal faces. We infer that the distinctive shapes and surfaces of xenocrystic olivine grains resulted from three distinct mechanical processes attending their rapid transport from their source in the mantle lithosphere: (1) penetrative flaking from micro-tensile failure induced by rapid decompression; (2) sustained abrasion and attrition arising from particle-particle collisions between grains in a turbulent, volatile-rich flow regime, and; (3) higher energy particle-particle collisions that produced impact cavities superimposed on decompression structures. The combination of these processes during the rapid ascent of kimberlite magmas is responsible for the distinctive ellipsoidal shape of olivine xenocrysts found in kimberlites worldwide.

1 Introduction

Kimberlite magmas, derived from very low partial melts of the mantle, erode, carry and erupt significant amounts of crystalline lithospheric mantle as whole rock nodules and as single crystals (e.g. Mitchell, 1986). They are consequently important geochemical and physical windows into the inner Earth. Abundant, sub-rounded to rounded, ovoid

SED

5, 2283–2312, 2013

The morphology and surface features

T. J. Jones et al.

Title Page

Abstract

Introduction

Conclusions

References

Tables

Figures

◀

▶

◀

▶

Back

Close

Full Screen / Esc

Printer-friendly Version

Interactive Discussion



The morphology and surface features

T. J. Jones et al.

Title Page

Abstract

Introduction

Conclusions

References

Tables

Figures

◀

▶

◀

▶

Back

Close

Full Screen / Esc

Printer-friendly Version

Interactive Discussion



to elliptical grains of xenocrystic mantle olivine are characteristic of kimberlite intrusions, lavas and pyroclastic rocks (e.g. Brett et al., 2009; Clement and Skinner, 1979, 1985; Dawson and Hawthorne, 1973; Gernon et al., 2012; Kamenetsky et al., 2008; Mitchell, 1986, 2008; Moss and Russell, 2011) although the origin of their ellipsoidal morphologies remains somewhat enigmatic given that they represent disaggregated crystalline rocks. Explanations include rounding by magmatic corrosion and dissolution of the grains during ascent, or milling (Brett et al., 2009; Brett, 2009; Reid et al., 1975; Russell et al., 2012). Rapid CO₂ release following digestion of orthopyroxene was recently proposed as a mechanism for propelling kimberlite magmas rapidly to the surface over short timescales (Russell et al., 2012). Such a process is potentially a significant factor in increasing the erosive potential of the ascending magmas at depth. Intuitively, chemical corrosion and milling should leave different physical signatures on the exteriors of mantle-derived crystals, which, if not overprinted by late stage crystal growth rims, or removed by alteration, should be discernible with scanning electron microscopy. Such features can provide insights into the nature of kimberlite magma transport from the mantle upwards: a topic still relatively poorly understood (e.g. Russell et al., 2012; Sparks, 2013; Sparks et al., 2006).

Here, we semi-quantitatively describe and analyse the shapes and surfaces of fresh xenocrystic olivine extracted from a Quaternary kimberlite lava in Tanzania. Our goals are two-fold: firstly, to understand the processes that create the highly distinctive shapes and surfaces of olivine crystals characteristic of kimberlite rocks; and secondly, to constrain ideas on the ascent of kimberlite magma.

2 Igwisi Hills volcanoes

The Quaternary Igwisi Hills monogenetic volcanoes (IHV), Tanzania, erupted at least $3.4 \times 10^7 \text{ m}^3$ of kimberlite magma, now mostly preserved as three small volcanic edifices: the NE, SW and central volcano (Brown et al., 2012). The $\sim 10 \text{ ka}$ IHV are the youngest kimberlite volcanoes on Earth; postdating the next youngest kimberlite volca-

noes by ~ 30 Ma (Brown et al., 2012). As a result of their young age, the deposits show remarkably low degrees of alteration. The IHV are located along a ~ 2 km NE–SW trending fissure (Fig. 1).

Brown et al. (2012) proposed three eruptive phases for the IHV: initial phreatomagmatic explosions were followed by weak eruptions columns and effusion of lava. Brown et al. (2012) estimated that the lava flows had relatively high effective viscosities at emplacement ($> 10^2$ to 10^6 Pa s); these are high compared to the range assumed for kimberlite magmas (~ 1 Pa s, e.g. Sparks et al., 2006). Higher viscosities are ascribed to the effects of shallow magma degassing and partial crystallization of the groundmass. Brown et al. (2012) also provided a lower limit on magma viscosity by modelling olivine settling, which suggested a partially crystallised Bingham-like fluid with a yield strength and viscosities of 10^3 Pa s.

Dawson (1994) showed that the IHV showed strong affinities to low alkali, calcite-rich kimberlites such as the Benfontein sills, South Africa. Reid et al. (1975), noted that the Igwisi material is characterised by ellipsoidal forsterite olivine hosted in a fine grained carbonate-apatite-spinel-perovskite-serpentine matrix. These xenocrysts and the polycrystalline xenoliths are ovoid and range up to 3 cm (i.e. “micro-xenoliths”; Dawson, 1994) In a few cases olivine ellipsoids are rimmed by or partially rimmed by pervoskite and Mg-Al spinel. Some olivine contains mineral inclusions including chrome pyrope, Mg-Al chromite, low Al enstatite, low Al magnesian chrome diopside and high Mg phlogopite (Reid et al., 1975). The olivine composition plots chemically in the kimberlite field; the olivine itself is forsterite rich and has a low Ca signature. Other mantle phases present in the micro-xenoliths provide estimates for pressure and temperature at formation. Under the assumption that the clinopyroxene coexisted with low Ca pyroxene, thermobarometry places the source temperatures at ~ 1000 °C (Davis and Boyd, 1966). Additionally, assuming chemical equilibrium, the coexistence of low Al_2O_3 enstatite with pyrope results in pressures of 50–60 kbar (Boyd, 1970).

The morphology and surface features

T. J. Jones et al.

Title Page

Abstract

Introduction

Conclusions

References

Tables

Figures

◀

▶

◀

▶

Back

Close

Full Screen / Esc

Printer-friendly Version

Interactive Discussion



3 Sample suite

In this study three sample sets were analysed. Individual olivine crystals from the Igwisi Hills (IH) lava are compared with olivines disaggregated from mantle xenoliths, and olivine phenocrysts from an Icelandic lava. Crystals disaggregated from mantle xenoliths can be used as a proxy for the original material prior to kimberlite ascent, whilst phenocrysts from the Icelandic lava illustrate surface textures of crystals crystallising from magma stored in the crust. Olivine from the IH lava, as opposed to the pyroclastic material, was used in this study to ensure that the surface textures were representative of the transport processes within the magma rather than, for example, explosive eruption processes. The secondary influence of subaerial eruption mechanisms can therefore be ignored.

3.1 Phenocrystic olivine

The picritic lava flow from Iceland contains abundant (> 20%) subhedral to euhedral forsteritic olivine phenocrysts with a grain size of approximately 2.5 mm. The sample was coarsely crushed to ~ 0.4–0.8 cm and then olivine grains were hand-picked under a binocular microscope. This allowed the crystals to be selected individually to avoid grains with unnatural breakage surfaces.

3.2 Mantle olivine

These samples comprise pristine lithospheric mantle-derived peridotitic xenoliths collected from a basanitic dike from Mt. Preston, western British Columbia (BC), Canada (Peterson, 2010). Detailed study of their mineralogy and textures shows that they record mantle equilibration conditions and have not been modified texturally or chemically during or post-emplacement (Peterson, 2010). As such, they provide a suitable reference material for the morphology of unadulterated mantle olivine. The peridotite

SED

5, 2283–2312, 2013

The morphology and surface features

T. J. Jones et al.

Title Page

Abstract

Introduction

Conclusions

References

Tables

Figures

◀

▶

◀

▶

Back

Close

Full Screen / Esc

Printer-friendly Version

Interactive Discussion



xenolith chosen was friable enough to disaggregate by hand. Olivine grains, 2–4 mm in diameter, were handpicked under a binocular microscope.

3.3 Igwisi Hills volcanoes

Large (1–10 mm) spheroidal olivine crystals make up a large proportion (~ 45 vol. %) of the lower parts of a pāhoehoe-type lava flow from the NE volcano at Igwisi Hills (Fig. 2a; Brown et al., 2012). They are rounded to sub-rounded in shape with typical aspect ratios of 1.5. The olivine grains were carefully removed by cutting out a small volume of lava with the olivine enclosed by a thin layer of groundmass. The fine groundmass readily disaggregated on rinsing with water. The sample surface was checked for attached groundmass with EDS prior to analysis. This ensured any dissolution, mechanical or etching features observed were solely the result of the volcanic or magmatic processes rather than the experimental method.

SEM/EDS analysis shows the IHV olivine crystals to be close to the forsterite end member of the olivine solid solution. Some margins of these rounded olivine grains contain smaller, ~ 0.2 mm sub-grains, which represent recrystallization from an original single olivine crystal (Fig. 2c). The peripheral olivine grains are randomly orientated but still retain the overall rounded shape, suggesting that recrystallization post-dates and conforms to the rounded structure. It is observed that recrystallization has occurred to variable degrees. Replacement occurs by strain-free elongate neoblasts around the periphery and is focused at the grain ends with maximum curvature (Fig. 2b and c). Several larger olivine grains contain small (< 1 mm) inclusions of spinel, clinopyroxene, garnet and/or apatite.

The groundmass of the host lava is very fine grained, and difficult to resolve well under a petrographic microscope. Small ~ 1 mm rounded olivine grains occur along with spinel and perovskite. Carbonate comprises up to 40 % of the groundmass material.

The morphology and surface features

T. J. Jones et al.

Title Page

Abstract

Introduction

Conclusions

References

Tables

Figures

◀

▶

◀

▶

Back

Close

Full Screen / Esc

Printer-friendly Version

Interactive Discussion



4 Methodology

4.1 Image analysis

Olivine is the dominant phase in kimberlite and therefore its abundance and grain size distributions are commonly used to characterise kimberlite units (e.g. Field et al., 2009; Jerram et al., 2009; Moss et al., 2010). The corresponding olivine grain size distribution for the IHV lava is shown in Fig. 3b. The grain size and shape distributions of olivine are based on a high resolution (1200 dpi) scan of a polished slab (Fig. 2a). The resulting digital image was manually traced using Adobe Illustrator to provide a representation of the slab outline and each olivine grain. Olivine grains in the IHV rocks vary from 1–10 mm in diameter. Manual tracing captured all olivine grains with long axes > 1.6 mm. The digital representation of the olivine grains within the slab (Fig. 3a) was analysed using ImageJ software (<http://rsbweb.nih.gov/ij/>) for geometric parameters including circularity, axis length and area.

4.2 Scanning electron microscopy

Hand-picked olivine grains from all three sample sets were mounted, carbon coated and studied under the Philips XL30 Scanning Electron Microscope (SEM) at the University of British Columbia to document surface textures observed across all sample suites.

4.3 3-D laser measuring microscopy

An Olympus LEXT 3-D Measuring Laser Microscope OLS4000 was used at the Advanced Materials and Process Engineering Laboratory (AMPEL), University of British Columbia, to collect data on the surface topography of the olivine grains. This device is calibrated in the same way as standard stylus instruments for surface measurements however it uses contactless measurement with an automatic line stitching function to create a topographic map at a high resolution. These data sets were used to create

The morphology and surface features

T. J. Jones et al.

Title Page

Abstract

Introduction

Conclusions

References

Tables

Figures



Back

Close

Full Screen / Esc

Printer-friendly Version

Interactive Discussion



models for the micron-scale topographic features of olivines from each of the three sample suites. The models were then used to make a quantitative comparison of the surface properties.

5 Results

5.1 Image analysis results

The cumulative frequency plot (Fig. 3b) shows the sphere-equivalent grain size plotted as a function of cumulative area percent. We have computed the Inman graphical standard deviation (σ_φ) as defined by:

$$\sigma_\varphi = (\varphi_{84} - \varphi_{16})/2 \quad (1)$$

to be 0.595 (Inman, 1952). On this basis, the olivine grains are very well sorted (Cas and Wright, 1987) presumably reflecting the relatively narrow range of olivine grain sizes in the cratonic mantle lithosphere and the small degree of mechanical attrition attending transport and eruption. We also calculated the circularity (C), a measure of roundness, for the olivine grains using:

$$C = 4\pi \left(A/P_{\text{Trace}}^2 \right) \quad (2)$$

where A and P_{Trace} are the area and the perimeter of individual olivine grains recovered by image analysis via ImageJ. A circularity value of 1 indicates a perfect circle and for all other shapes circularities are < 1 . As the value tends to 0, an increasingly elongated polygon is formed. Figure 3c shows a sharp peak in olivine circularity at ca. 0.85, nearly all IHV olivine grains show circularity values within a narrow range of 0.7 to 0.95. This quantifies the highly rounded nature to be well rounded and close to a circle.

Lastly, we define a new parameter of ellipticity (E), by Eq. (3):

$$E = P_{\text{R}}/P_{\text{Trace}} \quad (3)$$

The morphology and surface features

T. J. Jones et al.

Title Page

Abstract

Introduction

Conclusions

References

Tables

Figures

◀

▶

◀

▶

Back

Close

Full Screen / Esc

Printer-friendly Version

Interactive Discussion



Where P_R is the perimeter of a model ellipse which has the same major, a_{Trace} , and minor, b_{Trace} , axes as those measured on the olivine outline. The model ellipse is calculated by the Ramanujan's Approximation shown in Eq. (4) (Campbell, 2012; Ramanujan, 1962).

$$P_R = \pi \left(3 \left(\frac{a_{\text{Trace}}}{2} + \frac{b_{\text{Trace}}}{2} \right) - \sqrt{\left(\frac{3a_{\text{Trace}}}{2} + \frac{b_{\text{Trace}}}{2} \right) \left(\frac{a_{\text{Trace}}}{2} + \frac{3b_{\text{Trace}}}{2} \right)} \right) \quad (4)$$

Figure 3d shows the distribution of ellipticity values for the digitalised slab (Fig. 3a). For this parameter $E = 1$ is true for a perfect ellipse and all other values < 1 represent other shapes which deviate from a perfect ellipse. The olivine grains have a mean ellipticity of 0.935 and c. 97 % of the measured olivine grains have ellipticity values between 0.9 and 1.0. When comparing Fig. 3c and d it is clear that the olivine grains are better described in 2-D as an ellipse rather than a circle. Tables of values of circularity and ellipticity can be found in Appendix A.

5.2 Scanning electron microscopy

5.2.1 Phenocrystic olivine

Samples used for SEM imaging show little evidence of fractured surfaces resulting from the extraction of the crystals from the parent rock. They represent the primary surfaces of the olivine crystals which crystallised as a phenocryst phase from the basaltic melt. The overall crystal morphology is shown in Fig. 4a. Figure 4b and c shows a typical featureless surface at two different magnifications: it is very smooth, and flakes and pits are not present

5.2.2 Mantle olivine

SEM imaging confirms that these samples represent primary olivine surfaces that have not experienced alteration or unnatural fracturing during extraction from the host rock

The morphology and surface features

T. J. Jones et al.

Title Page

Abstract

Introduction

Conclusions

References

Tables

Figures

◀

▶

◀

▶

Back

Close

Full Screen / Esc

Printer-friendly Version

Interactive Discussion



The morphology and surface features

T. J. Jones et al.

Title Page

Abstract

Introduction

Conclusions

References

Tables

Figures

◀

▶

◀

▶

Back

Close

Full Screen / Esc

Printer-friendly Version

Interactive Discussion



±2 μm of the median surface. The contour map (Fig. 7c and d) for the mantle olivine shows a stepped appearance; all the measured mantle olivine surfaces show a decrease in surface elevation along the x-axis. The steps are sub-parallel to the y-axis and generate a decrease in topography of about 15 μm across the field of view; it is believed that these steps represent surfaces parallel to crystal faces exposed by minor flaking of the olivine crystals exterior (cf. SEM images in Fig. 5).

The IHV samples have a greater surface roughness than both the phenocrystic and mantle olivine grains (Fig. 7f). Contour maps for the IHV olivine (Fig. 7e) also record circular depressions of variable diameter; these are interpreted as the craters/pits observed under the SEM (Fig. 6b). The features are approximately 8–9 μm in depth with diameters of ~ 10–25 μm.

6 Discussion

6.1 Origin of IHV olivine surface features

All analysed samples of phenocrystic olivine show smooth, near featureless surfaces with zero topography. These surfaces are attributed to a free growth from a liquid melt. They show no similarities to the Igwisi Hills samples. Mantle olivine samples commonly display flaked surfaces and a stepped topography (Fig. 5c). However, at a larger scale the mantle olivine grains have sharply faceted, subhedral to euhedral shapes reflecting their textural equilibrium developed under the stable high temperature pressure conditions they formed at in the mantle. The micron-scale flaking is developed on, and post-dates, these sharply faceted crystal faces. These flaking structures are inferred to form during decompression when the crystal experiences lower pressures during ascent. The flakes are identical in chemistry to that of the surrounding fresh olivine (Fig. 5c). Therefore, they are related to decompression rather than to chemical reaction between the crystal and the melt. For example, there is no evidence of melt infiltration and reaction during transport within the mantle nodules, themselves (Peterson, 2010).

The morphology and surface features

T. J. Jones et al.

Title Page

Abstract

Introduction

Conclusions

References

Tables

Figures

◀

▶

◀

▶

Back

Close

Full Screen / Esc

Printer-friendly Version

Interactive Discussion



The IHV lava olivine grains display shapes and surface morphologies which are significantly different to the phenocrysts and the mantle nodules. We observe a highly flaked, irregular and rough surface with flakes penetrating internally; they are not just a superficial single layer feature (Fig. 6a). We interpret this penetrative multiple layer flaking to be a feature akin to exfoliation and related to decompression. The flaking structure has some similarities to the flaking observed in the mantle olivine. However on the IH samples flaking is pervasive, much more intense, occurs as multiple layers and it is a dominant feature on every IHV olivine analysed.

Similarities are expected considering these features are believed to be related to rapid decompression, both groups of olivine have been brought to the surface and are currently out of equilibrium with formation conditions. Olivine is incorporated into kimberlitic melts at great depths as peridotitic mantle xenoliths. Rapid ascent of 1–20 ms⁻¹ (Sparks et al., 2006) in the kimberlite system drives the xenoliths out of equilibrium with the surrounding pressure and temperature conditions resulting in decompression and expansion (Brett, 2009). Tensile cracks, within kimberlitic olivine, are known to occur during rapid ascent; they often occur in a parallel formation along cleavage planes (Hurrai et al., 2008; Tingle, 1988). Tensile failure occurs when the change in stress, coupled to ascent rate, experienced by the olivine crystal is greater than it can viscously relax, defining the tensile strength for kimberlite olivine (Brett, 2009). Given the ascent rates thought to occur in kimberlite deposits, crystals crack approximately 17 km above their source. This initial cracking event releases the maximum energy, although the crystals will continually crack from this point to surface levels (Brett, 2009).

Therefore it is hypothesised that the exfoliation features (Fig. 6) are a result of the outer surfaces of the crystal experiencing a stress differential, an expansion rate, faster than the timescales needed for viscous relaxation. Rapid decompression of solids can cause differential expansion of the clast rim vs. its interior. This produces tangential compression within the exterior rim and radial tension in the interior (Preston and White, 1934). We hypothesise that the stresses are partially released by exfoliation of the surface in a similar manner to thermal exfoliation (Preston and White, 1934; Thirumalai,

1969). These partial spalls would be easily removed via crystal-crystal collisions during turbulent transport, thereby enhancing the overall rates of attrition (Campbell et al., 2013).

5 Additionally the IHV olivine grains also have discrete depressions and impact pits. Figure 6b and c shows (semi) hemispherical cavities, they represent impact pits, produced by particle-particle collisions, similar to the abrasion process however involving higher energies (Campbell et al., 2013; Dufek et al., 2009, 2012). When comparing IHV olivine morphologies to an experimental abrasion data set (Kuenen, 1960) we hypothesise that the IHV olivine are resultant from at least ~ 25–45 % volume loss (Campbell et al., 2013).

6.2 Mechanical or chemical shaping

15 Olivine is well known to interact with kimberlitic melt during transport (e.g. Donaldson, 1990; Edwards and Russell, 1996, 1998). We therefore question to what extent the IHV olivine crystals have been modified by chemical processes rather than the mechanical processes described in this study. To investigate this, IHV olivine crystals were etched with 10 % hydrochloric acid on timescales varying from minutes to days. Their surfaces were then analysed under the SEM and compared to the natural samples.

20 Etch-pit formation by chemical dissolution is affected by the composition of the etchant, the crystal chemistry, crystallographic orientation, and the presence of impurities (“poisons”) in the etchant. This “poison” may enhance the selectivity of the etching surface (Wegner and Christie, 1974). Thus, our experiments are not intended to replicate exactly magmatic dissolution processes; rather they serve as an analogue for comparative purposes.

25 Figure 8a shows an experimentally etched Igwisi Hills lava olivine, at this scale it resembles all other IH olivine in the sample suite displaying numerous characteristic features shown in Fig. 6. However at higher magnifications (Fig. 8b) previously unidentified features become apparent on the olivine surface. The etched olivine shows elongate structures strongly controlled by the crystallographic structure of the olivine (Fig. 8c);

The morphology and surface features

T. J. Jones et al.

Title Page

Abstract

Introduction

Conclusions

References

Tables

Figures

◀

▶

◀

▶

Back

Close

Full Screen / Esc

Printer-friendly Version

Interactive Discussion



they do not resemble anything observed in the natural samples. Away from the main etch pit the original olivine surface has also been modified and is now more porous and exhibits a honeycomb-like texture; the natural surfaces of IHV olivine grains do not exhibit these textures.

We expect olivine to be subjected to both chemical and mechanical processes during transport. However the shapes and surfaces recorded within the erupted products studied are clearly dominated by mechanical processes; no similarities with the artificially etched samples are identified. We hypothesise that the chemical processes may dominate at greater depth (in the mantle lithosphere). Then, as the magma exsolves fluids and becomes more buoyant, its ascent velocity will rise. This results in a gas-rich mixture traveling at velocities that support turbulent flow and in which mechanical processes begin to dominate.

6.3 Implications for kimberlite ascent

Olivines from IHV lavas have elliptical morphologies and surfaces which preserve impact features that, to our knowledge, are unique. Importantly, these features must be the result of transport within the subsurface prior to eruption, because the olivine grains occur in a gently effused pāhoehoe-type lava. We propose a three part model to explain the distinctive attributes of the IHV olivine grains (Fig. 9). Firstly, olivine crystals become incorporated into a kimberlitic melt as whole rock mantle xenoliths. These xenoliths then undergo disaggregation facilitated by mineral expansion during ascent-driven continuous decompression. This imposes a build-up of internal stresses within the olivine crystal. The imposed timescales of ascent are faster than the olivine can viscously relax and the stresses are relieved by surface parallel micro-exfoliation (Brett, 2009). This results in the penetrative flaked surfaces observed.

Secondly, decompression makes the olivine more susceptible for abrasion through particle-particle collisions sustained within a rapidly ascending, volatile rich, turbulent mixture of solid, gas and melt driven by the assimilation of orthopyroxene (Russell et al., 2012). This gives rise to the final highly elliptical, near spherical morphologies docu-

The morphology and surface features

T. J. Jones et al.

Title Page

Abstract

Introduction

Conclusions

References

Tables

Figures

◀

▶

◀

▶

Back

Close

Full Screen / Esc

Printer-friendly Version

Interactive Discussion



mented. The hypothesis of abrasion producing rounding of angular clasts to spherical shapes is supported by experimental studies (Kuenen, 1960). Abrasion will exploit pre-existing weaknesses and preferentially erode weaker compounds (Suzuki and Takahashi, 1981).

5 Thirdly, higher energy particle-particle impacts create the hemispherical and semi-hemispherical impact pits (Fig. 6b and d) that are superimposed on the rounded and exfoliated olivine. These events are of lower frequency and only occur when olivine grains collide at high velocities. However, there is an upper limit to the collisional energy – they must be lower than the threshold required for crystal breakage (Dufek et al.,
10 2012).

The textures on the olivine grains at the Igwisi Hills volcanoes are unique; to our knowledge there is only one other study, Brett (2009), where similar textures and rounding have been briefly described. The features have not been observed on crystals from other mafic eruptions. This may result from the slower ascent rates and shallower melt
15 sources (60–80 km) of other mafic volcanic systems (e.g., basalt, basaltic, nepheleneite), which lead to lower rates of decompression and the build-up of lower tensile stresses within crystals during transport. Additionally, these magmas in general have lower average solid particle abundances, which reduces the frequency of particle interactions within a turbulent fluid. Lastly, the lower volatile component of non-kimberlitic
20 magmas may result in more viscous magmas that dampen the energy of colliding solid particles.

Xenoliths and xenocrysts of minerals other than olivine are rare within the IHV rocks. This can be explained by the high abrasion stability of olivine, which is second only to diamond (in decreasing order: diamond-pyrope-olivine-picroilmenite-apatite-kimberlite,
25 Afanas'ev et al., 2008). Therefore during rapid turbulent ascent other mantle mineral phases are less likely to survive, relative to olivine.

The morphology and surface features

T. J. Jones et al.

Title Page

Abstract

Introduction

Conclusions

References

Tables

Figures

◀

▶

◀

▶

Back

Close

Full Screen / Esc

Printer-friendly Version

Interactive Discussion



7 Conclusions

The shapes and surface textures of xenocrystic olivine grains extracted from a young kimberlite lava have been described and interpreted. The xenocrystic olivine grains are ellipsoidal, exhibit rough surfaces, covered with flakes and pits. These surface features differ significantly from both olivine phenocrysts and from olivine disaggregated from mantle nodules in the laboratory. A three part model is proposed to explain these differences. (1) During rapid CO₂-driven magma ascent, decompression results in parallel micro-exfoliation on the surface of the xenocrystic olivine grains. (2) Turbulent suspension of solid, gas and melt phases during ascent promotes abrasion that results in the highly elliptical and sub-spherical grain morphology. (3) High velocity particle-particle impacts result in impact pitting of the surface. Synthetic experiments rule out chemical dissolution and melt reabsorption as the causative process for rounding. The morphology and surface features of the xenocrystic olivine grains are consistent with mechanical processes operating during rapid CO₂-driven turbulent ascent of the magma from depth.

Supplementary material related to this article is available online at <http://www.solid-earth-discuss.net/5/2283/2013/sed-5-2283-2013-supplement.pdf>.

Acknowledgements. We would like to thank AMPEL for support with the Laser Measuring Microscope. JKR is supported by the NSERC Discovery Grants program. LP acknowledges support from a Marie Curie International Outgoing Postdoctoral Fellowship. Fieldwork on the Igwisi Hills Volcanoes was supported by a grant from National Geographic Committee for Research and Exploration awarded to RJB.

SED

5, 2283–2312, 2013

The morphology and surface features

T. J. Jones et al.

Title Page

Abstract

Introduction

Conclusions

References

Tables

Figures

◀

▶

◀

▶

Back

Close

Full Screen / Esc

Printer-friendly Version

Interactive Discussion



References

- Afanas'ev, V. P., Nikolenko, E. I., Tychkov, N. S., Titov, A. T., Tolstov, A. V., Kornilova, V. P., and Sobolev, N. V.: Mechanical abrasion of kimberlite indicator minerals: experimental investigations, *Russ. Geol. Geophys.*, 49, 91–97, 2008.
- 5 Boyd, F.: Garnet peridotites and the system $\text{CaSiO}_3\text{-MgSiO}_3\text{-Al}_2\text{O}_3$, *Mineral. Soc. Amer. Spec. Pap.*, 3, 63–75, 1970.
- Brett, R. C.: Kimberlitic olivine, M.S. thesis, University of British Columbia, Columbia, 2009.
- Brett, R. C., Russell, J. K., and Moss, S.: Origin of olivine in kimberlite: phenocryst or impostor?, *Lithos*, 112, 201–212, 2009.
- 10 Brown, R. J., Many, S., Buisman, I., Fontana, G., Field, M., Mac Niocaill, C., Sparks, R., and Stuart, F.: Eruption of kimberlite magmas: physical volcanology, geomorphology and age of the youngest kimberlitic volcanoes known on earth (the Upper Pleistocene/Holocene Igwisi Hills volcanoes, Tanzania), *B. Volcanol.*, 74, 7, 1621–1643, 2012.
- Campbell, M.: Thermomechanical milling of lithics in volcanic conduits, M.S. thesis, University of British Columbia, Columbia, 2012.
- 15 Campbell, M. E., Russell, J. K., and Porritt, L. A.: Thermomechanical milling of accessory lithics in volcanic conduits, *Earth Planet. Sc. Lett.*, 377/378, 276–286, 2013.
- Cas, R. A. and Wright, J. V.: *Volcanic Successions, Modern and Ancient: a Geological Approach to Processes, Products, and Successions*, Allen and Unwin, 1987.
- 20 Clement, C. and Skinner, E.: A textural genetic classification of kimberlite rocks, *Kimberlite Symposium II*, Cambridge, in: *Proceedings Extended Abstracts*, 1979.
- Clement, C. and Skinner, E.: A textural-genetic classification of kimberlites, *S. Afr. J. Geol.*, 88, 403–409, 1985.
- Davis, B. and Boyd, F.: The join $\text{Mg}_2\text{Si}_2\text{O}_6\text{-CaMgSi}_2\text{O}_6$ at 30 kilobars pressure and its application to pyroxenes from kimberlites, *J. Geophys. Res.*, 71, 3567–3576, 1966.
- 25 Dawson, J.: Quaternary kimberlitic volcanism on the Tanzania Craton, *Contrib. Miner. Petrol.*, 116, 473–485, 1994.
- Dawson, J. B. and Hawthorne, J. B.: Magmatic sedimentation and carbonatitic differentiation in kimberlite sills at Benfontein, South Africa, *J. Geol. Soc. London*, 129, 61–85, 1973.
- 30 Donaldson, C.: Forsterite dissolution in superheated basaltic, andesitic and rhyolitic melts, *Mineral. Mag.*, 54, 67–74, 1990.

The morphology and surface features

T. J. Jones et al.

Title Page

Abstract

Introduction

Conclusions

References

Tables

Figures

◀

▶

◀

▶

Back

Close

Full Screen / Esc

Printer-friendly Version

Interactive Discussion



The morphology and surface featuresT. J. Jones et al.

[Title Page](#)[Abstract](#)[Introduction](#)[Conclusions](#)[References](#)[Tables](#)[Figures](#)[◀](#)[▶](#)[◀](#)[▶](#)[Back](#)[Close](#)[Full Screen / Esc](#)[Printer-friendly Version](#)[Interactive Discussion](#)

Dufek, J., Wexler, J., and Manga, M.: Transport capacity of pyroclastic density currents: Experiments and models of substrate-flow interaction, *J. Geophys. Res.-Sol. Ea.*, 114, 1–13, 2009.

Dufek, J., Manga, M., and Patel, A.: Granular disruption during explosive volcanic eruptions, *Nature Geosci.*, 5, 561–564, 2012.

Edwards, B. and Russell, J.: A review and analysis of silicate mineral dissolution experiments in natural silicate melts, *Chem. Geol.*, 130, 233–245, 1996.

Edwards, B. R. and Russell, J. K.: Time scales of magmatic processes: new insights from dynamic models for magmatic assimilation, *Geology*, 26, 1103–1106, 1998.

Field, M., Gernon, T. M., Mock, A., Walters, A., Sparks, R. S. J., and Jerram, D. A.: Variations of olivine abundance and grain size in the Snap Lake kimberlite intrusion, Northwest Territories, Canada: a possible proxy for diamonds, *Lithos*, 112, 23–35, 2009.

Gernon, T., Field, M., and Sparks, R.: Geology of the Snap Lake kimberlite intrusion, Northwest Territories, Canada: field observations and their interpretation, *J. Geol. Soc. London*, 169, 1–16, 2012.

Hurai, V., Prochaska, W., Lexa, O., Schulmann, K., Thomas, R., and Ivan, P.: High-density nitrogen inclusions in barite from a giant siderite vein: implications for Alpine evolution of the Variscan basement of Western Carpathians, Slovakia, *J. Metamorph. Geol.*, 26, 487–498, 2008.

Inman, D. L.: Measures for describing the size distribution of sediments, *J. Sediment. Res.*, 22, 125–145, 1952.

Jerram, D. A., Mock, A., Davis, G. R., Field, M., and Brown, R. J.: 3-D crystal size distributions: a case study on quantifying olivine populations in kimberlites, *Lithos*, 112, 223–235, 2009.

Kamenetsky, V. S., Kamenetsky, M. B., Sobolev, A. V., Golovin, A. V., Demouchy, S., Faure, K., Sharygin, V. V., and Kuzmin, D. V.: Olivine in the Udachnaya-East kimberlite (Yakutia, Russia): types, compositions and origins, *J. Petrol.*, 49, 823–839, 2008.

Kuenen, P. H.: Experimental abrasion 4: eolian action, *J. Geol.*, 68, 427–449, 1960.

Mitchell, R. H.: Kimberlites: Mineralogy, Geochemistry, and Petrology, Plenum Press, New York, 1986.

Mitchell, R. H.: Petrology of hypabyssal kimberlites: relevance to primary magma compositions, *J. Volcanol. Geoth. Res.*, 174, 1–8, 2008.

Moss, S. and Russell, J.: Fragmentation in kimberlite: products and intensity of explosive eruption, *B. Volcanol.*, 73, 983–1003, 2011.

- Moss, S., Russell, J. K., Smith, B. H. S., and Brett, R. C.: Olivine crystal size distributions in kimberlite, *Am. Mineral.*, 95, 527–536, 2010.
- Preston, F. W. and White, H. E.: Observations on spalling*, *J. Ceram. Soc.*, 17, 137–144, 1934.
- Peterson, N. D.: Carbonated mantle lithosphere in the western Canadian Cordillera, M. S. thesis, University of British Columbia, Columbia, 2010.
- Ramanujan, S.: *Ramanujan's Collected Works*, New York, Chelsea, 1962.
- Reid, A. M., Donaldson, C., Dawson, J., Brown, R., and Ridley, W.: The Igwisi Hills extrusive “kimberlites”, *Phys. Chem. Earth*, 9, 199–218, 1975.
- Russell, J. K., Porritt, L. A., Lavallée, Y., and Dingwell, D. B.: Kimberlite ascent by assimilation-fuelled buoyancy, *Nature*, 481, 352–356, 2012.
- Sparks, R.: Kimberlite volcanism, *Annu. Rev. Earth Pl. Sc.*, 41, 497–528, 2013.
- Sparks, R., Baker, L., Brown, R., Field, M., Schumacher, J., Stripp, G., and Walters, A.: Dynamical constraints on kimberlite volcanism, *J. Volcanol. Geoth. Res.*, 155, 18–48, 2006.
- Suzuki, T. and Takahashi, K. I.: An experimental study of wind abrasion, *J. Geol.*, 89, 509–522, 1981.
- Thirumalai, K.: Process Of Thermal Spalling Behavior In Rocks An Exploratory Study, in: *Proceedings The 11th US Symposium on Rock Mechanics (USRMS)*, 1969.
- Tingle, T. N.: Retrieval of uncracked single crystals from high pressure in piston-cylinder apparatus, *Am. Mineral.*, 73, 1195–1197, 1988.
- Wegner, M. and Christie, J.: Preferential chemical etching of terrestrial and lunar olivines, *Contrib. Miner. Petrol.*, 43, 195–212, 1974.

The morphology and surface features

T. J. Jones et al.

Title Page

Abstract

Introduction

Conclusions

References

Tables

Figures

◀

▶

◀

▶

Back

Close

Full Screen / Esc

Printer-friendly Version

Interactive Discussion



The morphology and surface features

T. J. Jones et al.

Title Page

Abstract

Introduction

Conclusions

References

Tables

Figures

◀

▶

◀

▶

Back

Close

Full Screen / Esc

Printer-friendly Version

Interactive Discussion

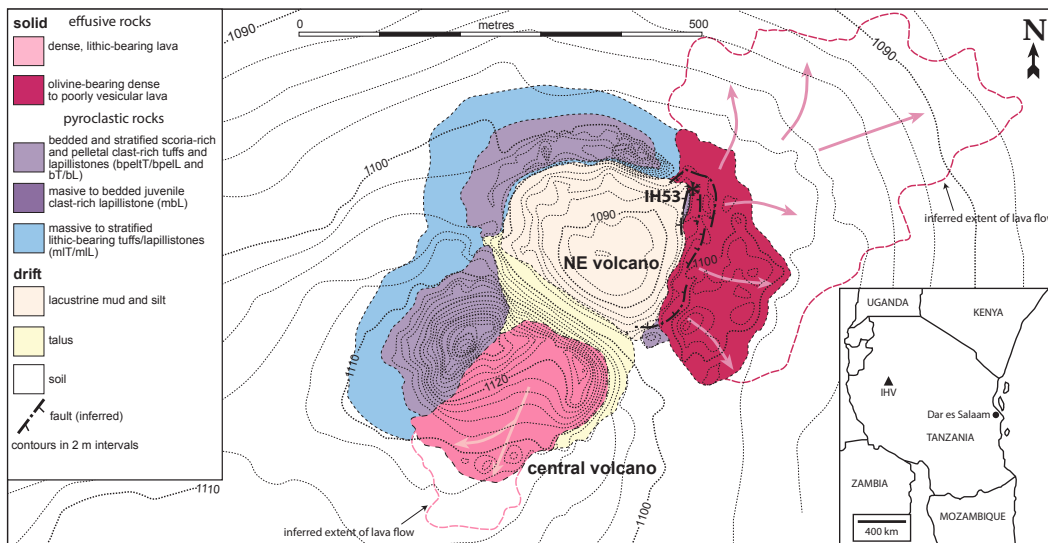


Fig. 1. Map of Igwisi Hills volcanoes, showing the relative positions of the two northernmost volcanic edifices and the location of the lava (IH53) sampled in this study. The Igwisi Hills volcanoes are situated at latitude $4^{\circ}51' S$, and longitude $31^{\circ}55' E$. Adapted from Brown et al. (2012).

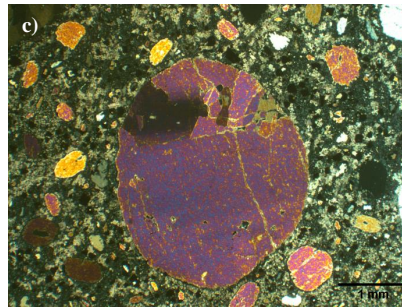
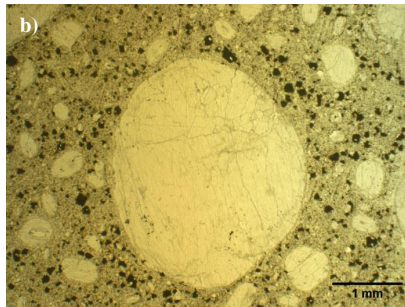


Fig. 2. Xenocrystic olivine grains within Igwisi Hills lava sample IH53. **(a)** High resolution scan of polished slab of lava sample showing abundance, distribution and highly ellipsoidal shapes of xenocrystic olivine. **(b)** Photomicrograph under plane polarized light of Igwisi Hills lava sample studied by Dawson (1994). **(c)** Photomicrograph under crossed polarized light of same thin section **(b)**, showing the development of sub grains whilst retaining an ellipsoidal shape.

The morphology and surface features

T. J. Jones et al.

Title Page

Abstract

Introduction

Conclusions

References

Tables

Figures

◀

▶

◀

▶

Back

Close

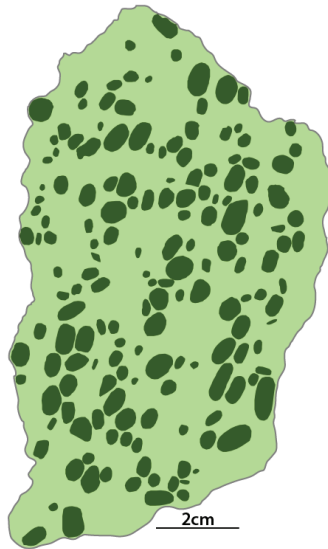
Full Screen / Esc

Printer-friendly Version

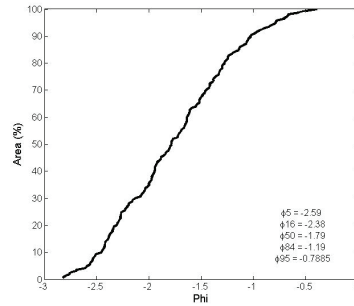
Interactive Discussion



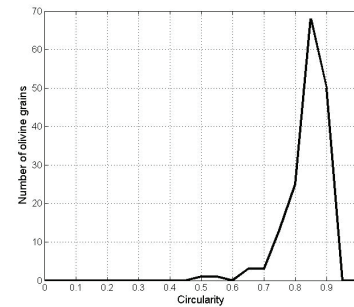
a)



b)



c)



d)

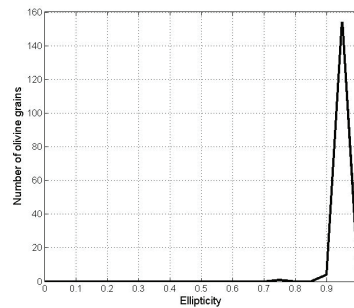


Fig. 3. Caption on next page.

SED

5, 2283–2312, 2013

The morphology and surface features

T. J. Jones et al.

Title Page

Abstract

Introduction

Conclusions

References

Tables

Figures

◀

▶

◀

▶

Back

Close

Full Screen / Esc

Printer-friendly Version

Interactive Discussion



SED

5, 2283–2312, 2013

The morphology and surface features

T. J. Jones et al.

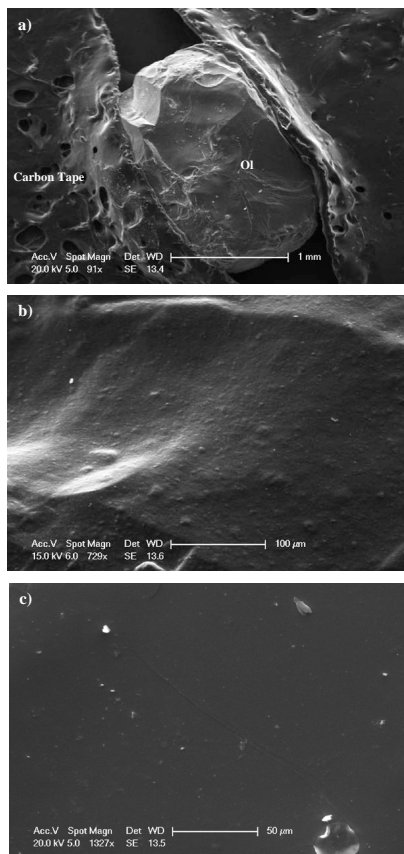


Fig. 4. SEM imagery for an olivine phenocryst from an Icelandic picritic basalt lava. **(a)** Olivine grain bounded by mounting tape showing overall morphology of crystal grown from melt. **(b)** and **(c)** Detailed images of primary surfaces (unfractured) typical of phenocrystic olivine which shows minimal topography.



The morphology and surface features

T. J. Jones et al.

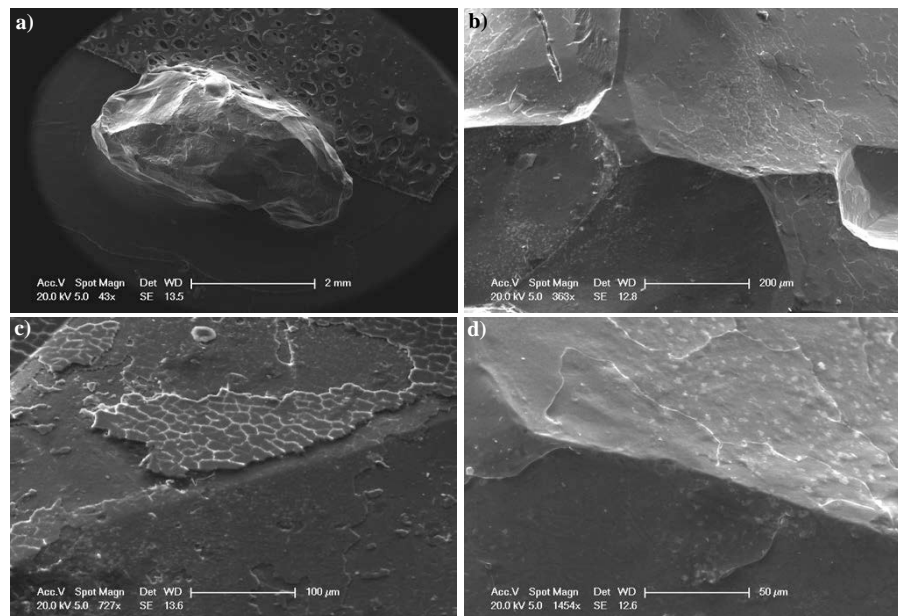


Fig. 5. SEM imagery for an olivine grain from mantle-derived peridotite. **(a)** Olivine grain bounded by mounting tape (top) showing overall shape of grain. **(b)** Detailed image of primary surface (unfractured) of olivine typical of grains forming an interlocking mosaic within mantle peridotite. **(c)** Polygonal textured surface flaking **(d)** common small scale surface flakes on the mantle olivine surface. Higher relief is observed at the edge of the flake creating a stepped topography.

[Title Page](#)[Abstract](#)[Introduction](#)[Conclusions](#)[References](#)[Tables](#)[Figures](#)[◀](#)[▶](#)[◀](#)[▶](#)[Back](#)[Close](#)[Full Screen / Esc](#)[Printer-friendly Version](#)[Interactive Discussion](#)

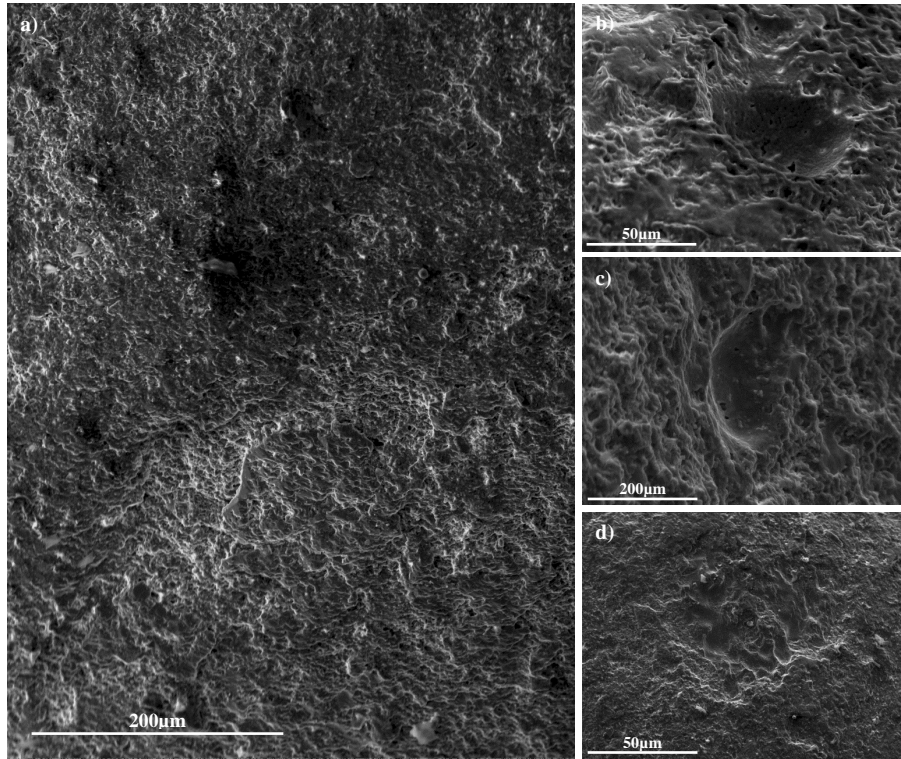


Fig. 6. SEM imagery for Igwisi Hills lava olivine. **(a)** Large scale image showing distinctive surface texture. **(b)** Hemispherical impact cavity featuring a smooth interior. **(c)** Several semi-hemispherical excavations, the edge of this attrition feature demonstrates penetrative multiple layer flaking of the olivine surface. **(d)** A common semi-hemispherical impact pit, again having a smooth interior.

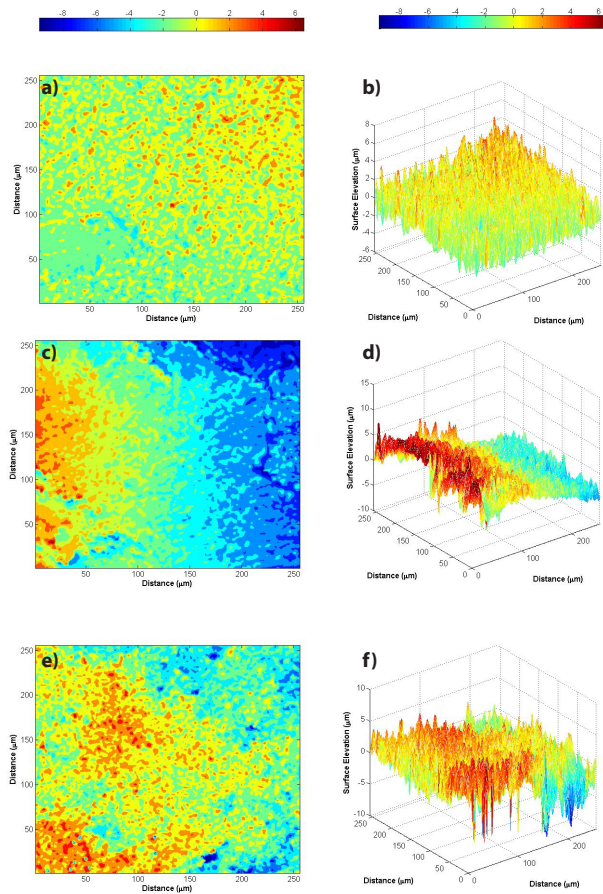


Fig. 7. Caption on next page.

The morphology and surface features

T. J. Jones et al.

Title Page

Abstract

Introduction

Conclusions

References

Tables

Figures

◀

▶

◀

▶

Back

Close

Full Screen / Esc

Printer-friendly Version

Interactive Discussion



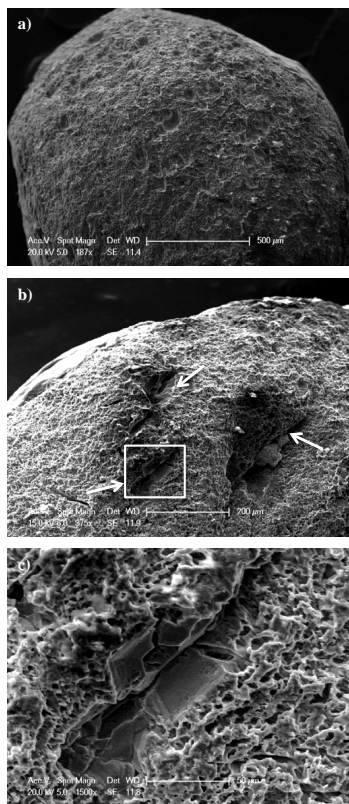


Fig. 8. SEM imagery of olivine surfaces subjected to dissolution by weak acids (see text). **(a)** Overall morphology of etched grain. **(b)** Detailed image of etched olivine surface; white arrows highlight etch pits. The white box shows the area represented by part c. **(c)** An etch pit developed on original surface of Igwisi Hills olivine; dissolution pit shape is strongly controlled by the crystallographic structure of the olivine.

The morphology and surface features

T. J. Jones et al.

Title Page

Abstract

Introduction

Conclusions

References

Tables

Figures

◀

▶

◀

▶

Back

Close

Full Screen / Esc

Printer-friendly Version

Interactive Discussion



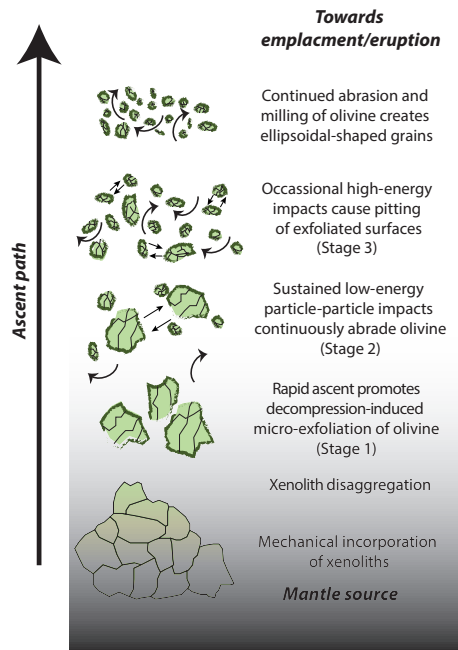


Fig. 9. Summary model for the evolution of olivine during ascent of kimberlite. Kimberlite ascent processes cause brittle deformation of mantle peridotite leading to production and entrainment of mantle xenoliths. Peridotitic xenoliths undergo mechanical disaggregation due to particle-particle collisions and decompression. The decompression is driven by rapid ascent and promotes tensile failure in liberated olivine crystals and is expressed as surface parallel micro-exfoliation. High velocity (i.e. turbulent) transport of olivine in a solids-rich melt-gas mixture of kimberlite magma supports continual high-frequency low energy impacts between particles leading to abrasion and rounding of olivine grains. Periodic higher-energy impacts create impact pits on the olivine's exfoliated surfaces. The combination of these processes results in a high proportion of ellipsoidal-shaped, abraded and decompressed olivine grains within the IH lavas.